

# In-situ analysis of phase formations in semi-solid state in the hypereutectic Al-Si alloy

A. V. Mazur, M. M. Gasik\*

*Helsinki University of Technology – TKK, FIN-02015 TKK, Helsinki, Finland*

Received 31 October 2007, received in revised form 1 February 2008, accepted 4 February 2008

## Abstract

Binary hypereutectic Al-21.5wt.%Si alloy was studied by XRD *in-situ* at 610°C in the two-phase (liquid + solid) state. Primary  $\beta$ -Si, liquid and  $\alpha$ -Al FCC phases were found to co-exist at 610°C. The  $\alpha$ -Al solid solution with FCC lattice parameter  $423.8 \pm 5$  pm was stably present in the hypereutectic melt over a long time soaking, although theoretical equilibrium phase diagram does not allow such combination. The total driving force of nucleation for classical Gibbs-Thomson and modified theories was calculated. The stable existence of  $\alpha$ -Al phase was explained as a kinetic effect due to local nucleation of silicon phase and it was shown to be thermodynamically favourable within certain limits of the nuclei size due to local depletion of the liquid phase when nucleation rate exceeds mass transport rate.

**Key words:** aluminium-silicon alloy, semi-solid state, crystal lattice, heterogeneous nucleation, Gibbs energy

## 1. Introduction

The phase formation during solidification of metallic melts is an essential process, which determines the final microstructure and properties of alloys. The solidification of melts with more than one component usually proceeds through a semi-solid range of liquid and solid (unless the composition is purely eutectic one) where high-temperature phase forms the first under liquidus curve.

It is generally assumed that the equilibrium state of the system is being approached during longer isothermal processing with constant parameters like pressure, total composition, etc. From the phase diagram analysis three main answers are usually being sought: the amount of equilibrium phases, fractions of these phases and the equilibrium concentrations of components in these phases. It is also generally known that solidification process is essentially non-equilibrium one and thus thermodynamically stable state should be considered as the final target but hardly achievable. Nevertheless, phase nucleation and growth are governed by thermodynamics which specific form of equations depends on the nucleation mechanism and other limiting factors like mass and heat transfer. Therefore,

by undercooling the melt below the liquidus and holding it isothermally at this temperature, one should be able to reach near-equilibrium state with some primary crystals and remaining liquid phase. In the case of Al-Si melts, these are primary  $\beta$ -Si phase which consists of mostly silicon and Al-Si liquid with composition defined by the liquidus point at this temperature [1–3]. However, because of possible different nucleation and phase growth kinetics the real state of the melt could be different from that prescribed by equilibrium thermodynamics. In this work the solid phases formation was studied in semi-solid state of the Al-21.5wt.%Si alloy at 610°C with *in-situ* XRD technique.

## 2. Experimental procedure

The experimental alloy was prepared of aluminium (99.99 %) and single crystal non-doped semiconductor grade silicon. The components were heated up to 1037°C until complete melting in an electrical resistance furnace in re-crystallized alumina crucible, soaked during 15 min and cooled with crucible. The ingot was partitioned into the samples for XRD and mi-

\*Corresponding author: tel.: +358 9 4512769; fax +358 9 4512799; e-mail address: [mgasik@pop.hut.fi](mailto:mgasik@pop.hut.fi)

Table 1. The interferences of  $\alpha$ -Al phase in the sample No. 1

<i>hkl</i>	111	200	220	311	222	400	331	420	422	511; 333	440
21 <sub>exp</sub> , E	16.70	19.20	27.60	–	–	39.19	42.86	44.08	48.32	51.22	56.31
21 <sub>calc</sub> , E	16.70	19.31	27.44	32.29	33.77	39.19	42.87	44.04	48.50	51.65	56.63

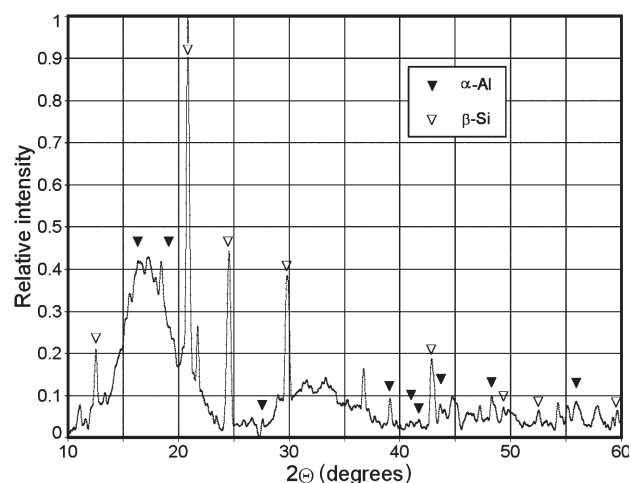


Fig. 1. The XRD patterns of Al-21.5wt.%Si alloy at 610°C for first soaking.

crostructural examinations. Sample No. 1 was studied with X-ray  $\Theta$ - $\Theta$  diffractometer by heating up to 830°C in-situ, soaking 30 min, cooling to  $610 \pm 2^\circ\text{C}$ , soaked 2.5 h at this temperature and after that analysed with XRD (Mo  $K\alpha$  radiation, scan rate  $2 \text{ deg min}^{-1}$ ) three times. Sample No. 1 has also been subjected to the same heating regime but after soaking at 610°C it was immediately quenched in 5 % acetic acid ice-water solution within a thin-walled (0.3 mm) alumina crucible. Estimated cooling rates were  $\sim 10^3 \text{ K s}^{-1}$ . This sample was used for microstructural examination (carried out with microscope Olympus PMG-3).

### 3. Results and discussion

The equilibrium phase diagram of the Al-Si system predicts the volume fraction of the liquid phase  $\sim 87\%$  at 610°C, the rest being  $\beta$ -Si solid phase (primary crystals). Figure 1 shows obtained XRD patterns (main contribution from liquid phase has been deducted because it was not the object of this study). There were practically no differences in patterns intensity and diffraction angles between the XRD measurements.

The positions of the  $\beta$ -Si phase peaks are slightly displaced vs. standard (room temperature) reference card data, probably as the result of the silicon lattice thermal expansion and some aluminium solubil-

ity. The interferences of the FCC lattice (solid solution of Si in Al-lattice, i.e.  $\alpha$ -Al phase) with lattice parameter  $423.8 \pm 5 \text{ pm}$  were also evident from the Fig. 1 (their identification is shown in Table 1). This lattice parameter reasonably agrees with reference parameter from CaRIne v.3.1 database corrected to thermal expansion of pure aluminium at 610°C ( $410.5 \pm 5 \text{ pm}$ ).

The microstructure of sample No. 1 includes typical primary silicon crystals (length 50, ..., 100  $\mu\text{m}$ , microhardness  $H_\mu = 8400\text{--}8800 \text{ MPa}$ ) and rounded bright-etching grains ( $H_\mu = 350 \text{ MPa}$ ) proven to be the  $\alpha$ -Al solid FCC solution (Table 1). These grains are only located at the surface and near the silicon crystals, forming nearly continuous shells around the silicon-rich crystal. The liquid phase of this sample is transformed into a fine-differentiated quasi-eutectic (Fig. 2a).

The essential difference of the microstructure between samples No. 1 (quenched from 610°C, Fig. 2a) and No. 2 (as-cast, Fig. 2b) is the absence of plate-like eutectic  $(\alpha\text{-Al} + \beta\text{-Si})_{\text{eut}}$  in the sample No. 1. The appearance of  $\alpha$ -Al (peaks in the XRD patterns and large rounded  $\alpha$ -grains) in the quenched sample is not expected from the equilibrium phase diagram. The possible obvious explanations are either that a) the equilibrium was not reached or b) the formation of the  $\alpha$ -phase is caused by some kinetics and mass transfer processes (due to isothermal conditions, the rate of the latent heat of solidification was assumed negligible). Few hours of soaking of any melt in isothermal conditions are in most cases rather long times for the composition and structure to equilibrate or at least to reach a near-equilibrium state. The formation of the  $\alpha$ -phase in hypereutectic Al-Si alloys could happen during quenching where mass transfer is suppressed. However, the differentiation of  $\alpha$ -phase grains branches is by an order less than the spacing between coarse rounded  $\alpha$ -grains at the surface of primary silicon crystals. This does not explain why  $\alpha$ -phase diffraction patterns exist in a stable way already at 610°C in the semi-solid state.

The performed XRD experiments clearly prove the formation of both solid  $\beta$ -Si and  $\alpha$ -Al in the hypereutectic alloy at 610°C at the same time. The patterns from the  $\alpha$ -phase were not changing with time what indicates the process to be at least in a steady state. The Al-Si melts are known to be microheterogeneous with a strong interaction in liquid state [1–4]. Independent in-situ analysis has indicated formation

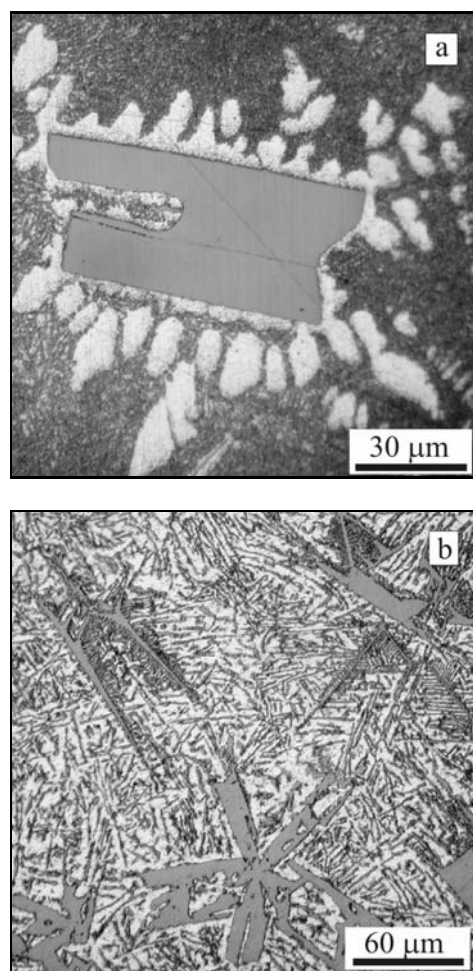


Fig. 2. Microstructure of Al-21.5%Si alloy (a – sample No. 1, b – sample No. 2).

of  $(-Si_4-Si_4-)$  clusters in near-eutectics hypereutectic alloys above the liquidus line [5]. The change of interaction type to  $(-Al_3Si-)$  in the melts as a result of increase of silicon above 17 % has also been shown earlier [1–3].

The formation of “extra-equilibrium” phases is widely observed in casting practice. In chill-cast Al-Si alloys, primary silicon crystals are normally surrounded by  $\alpha$ -phase. Excess silicon particles also appear in cast hypoeutectic alloys such as A356 [6], which is “impossible” according to the classical eutectic phase equilibrium diagram. During thixomolding of Al-(20, ..., 40)%Si alloys stable co-existence of  $\alpha$ -, liquid and  $\beta$ -phases was observed as well [7].

Formation of  $\beta$ -Si was described by theories involving both homogenous and heterogeneous nucleation [6, 8–10]. For homogenous nucleation the driving force is the negative free energy composed of volumetric Gibbs energy change due to a formation of over-critical nucleus and surface energy change due to formation of new interface between solid and liquid

phase (the Gibbs-Thomson equation) [11, 12]. Hillert and Rettenmayr [12] have shown that in any case the formation of solid phase leads to immediate depletion of the surrounding liquid phase so the equilibration of this zone with the bulk liquid towards new composition will take some time. The flux of species to be nucleated should be balanced with the reverse flux of the species stay in liquid state since no pores may exist in liquid phase [12]. With this approach, Wasai and Mukai [9] have analysed homogeneous nucleation of alumina from liquid Fe-Al-O system and have incorporated also change of the free energy of liquid phase that surrounds the nuclei. They have shown that this change may be significant to alter the classical free energy change of the Gibbs-Thomson equation. The situation in real metallurgical systems indeed differs from classical Gibbs or LSW theories due to space-limited nature of the samples where nuclei (although still could be considered as independent one) do affect remaining liquid which could not anymore be considered of constant liquidus composition. After the first nuclei were formed, the liquid zone composition, depleted by the solid phase components, might become favourable for heterogeneous nucleation of another phase(s), which might look “impossible” from the point of equilibrium phase diagram [10, 13].

To check the influence of the liquid free energy changes on thermodynamic driving force for the nucleation, a simple estimation was made using the similar approach as in [9, 12] with data for Al-Si alloys taken from [8], except those of Gibbs energies of pure Al and Si as well as for their solutions, which were taken from the ThermoCalc (version R) binary alloys database. Some additional surface energy data were taken from [14, 15]. The driving force for any stage and type of nucleation includes a) volumetric term, depending on supersaturation (specific undercooling), b) surface term, depending on creation of new interface between solid and liquid and c) a “halo” zone term, depending on the free energy change for the remaining local liquid due to its depletion by solidifying component. Here latent heat of crystallization and local heating/cooling effects are not considered and the system is supposed to be isothermal as it was in the recent experiments.

The Gibbs energy of  $\alpha$ -,  $\beta$ - and liquid phases at 610°C is shown in Fig. 3 for the whole composition range and in Fig. 4 enlarged for the range  $X_{Si} = 0, \dots, 0.25$ . Tangent lines  $dG/dX$  are plotted for  $\alpha$ -phase composition with  $X^\alpha = 0.011$  and for liquid with  $X^L = 0.209$  (as starting liquid composition), as could be retrieved from the well-known equilibrium Al-Si phase diagram. It could be seen (Fig. 3) that the initial liquid with  $X^L = 0.209$  cuts the line of  $\beta$ -phase free energy at  $X \sim 0.925$ , making formation of  $\beta$ -phase with 0, ..., 7.5 % Al thermodynamically possible [12]. This tangent line does not touch, however, the Gibbs energy curve of  $\alpha$ -phase, making this volumetric driving force

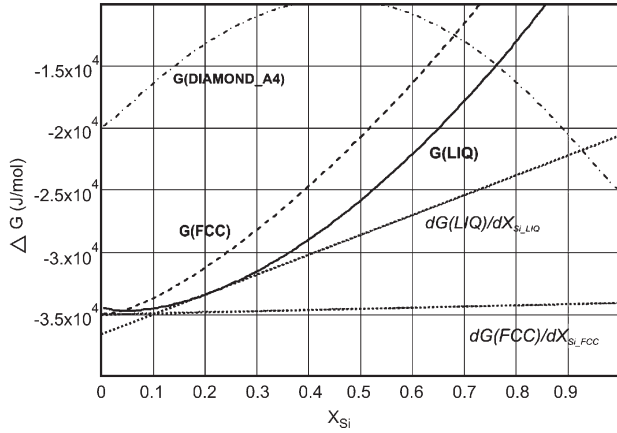


Fig. 3. Gibbs energy ( $\text{J mol}^{-1}$ ) of the main phases at  $610^\circ\text{C}$  with tangent lines (see text).

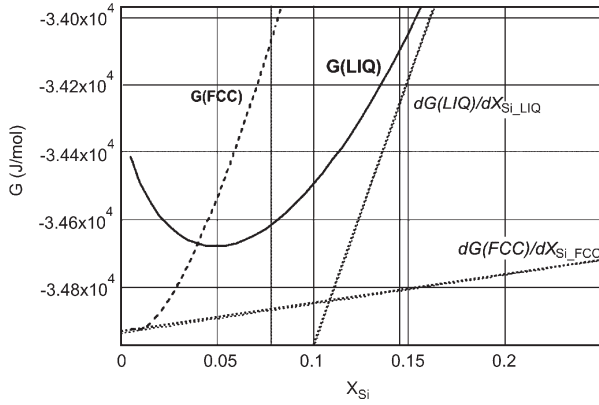


Fig. 4. Gibbs energy ( $\text{J mol}^{-1}$ ) of the main phases at  $610^\circ\text{C}$  (enlarged Al-corner of Fig. 3). Note very small range of minimal Gibbs energy of  $\alpha$ -phase.

for  $\alpha$ -nucleation too positive, as one may expect. From Fig. 4 one may also retrieve that absolute minimum (equilibrium value [12]) of the liquid phase is reached at  $X_e^L = 0.049$  and of the  $\alpha$ -phase at  $X_e^\alpha = 7.735 \times 10^{-3}$  at this temperature. These values present theoretical limits of reachable compositions of the respective phases [12], although this does not mean they may be practically achievable macroscopically in real systems.

It is now possible to calculate all these contributions for the nucleation driving force. For 1 mol of alloy, the number of nucleation sites might be taken as  $n_0 = 10^{13}$  or  $\sim 10^{18}$   $\beta$ -nuclei  $\text{m}^{-3}$  [9]. This means that every cubic volume with  $\sim 2\text{--}3 \mu\text{m}$  size would have at least one  $\beta$ -Si nucleation site (any realistic number  $n_0$  could be taken, but it affects only some numerical values without jeopardizing theoretical consideration below). As in a classical case, the first volumetric driv-

ing force could be written as

$$\Delta G_{\text{vol}} = n_0 \frac{4\pi}{3V_\beta^m} r^3 \Delta\mu_{\text{Si}}, \quad (1)$$

where  $r$  is the average radius of nucleus (m),  $V_\beta^m$  is molar volume of the phase ( $\text{m}^3 \text{mol}^{-1}$ ),  $\Delta\mu$  is actual local supersaturation degree (in this case the difference between chemical potentials of Si in solid  $\beta$ -phase and the liquid), ( $\text{J mol}^{-1}$ ). The second driving force contribution (surface term) is also similar to the classical case:

$$\Delta G_{\text{surf}} = n_0 4\pi r^2 \sigma_{\text{Si-L}}(r), \quad (2)$$

where  $\sigma_{\text{Si-L}}$  is surface energy at the  $\beta$ -phase and liquid interface ( $\text{J m}^{-2}$ ). It could also depend on the radius of nucleus (curvature) as suggested in [9]:

$$\sigma(r) = \frac{\sigma^0}{1 + \frac{r}{\Gamma}}; \quad \Gamma = \sqrt[3]{\frac{1}{N_A(V^m)^2}} \quad (3)$$

with  $\sigma^0$  is surface energy of the perfectly flat Si-liquid interface ( $\text{J m}^{-2}$ ),  $N_A$  is Avogadro's number and  $\Gamma$  is surface excess term ( $\text{mol m}^{-2}$ ) [9]. Here possible anisotropy of surface energy of nucleus is not considered. The third term of the driving force is calculated as change of the Gibbs energy of surrounding liquid [9]. At the time  $t = 0+$  (immediately after instant nucleation) number of moles of Si, remaining in the surrounding liquid zone will be:

$$n_{1,\text{Si}}(r) = N_0 X_{\text{Si}}^0 - n_0 \frac{4\pi}{3V_\beta^m} r^3 X_{\text{Si}}^\beta, \quad (4)$$

where  $N_0 = 1 \text{ mol}$  is initial amount of melt,  $X_{\text{Si}}^0 = 0.209$  is initial molar fraction of Si in the melt,  $X_{\text{Si}}^\beta = 0.995$  is the average Si molar fraction in the nucleating  $\beta$ -Si liquid enriches with aluminium and depletes with silicon, forming its new local composition ( $X_{1,\text{Si}}^L$ ). The thickness of the depleted zone and its exact composition depend on the mobility of silicon and aluminium, possible trans-interface diffusion, energy and mass balances [12]. The change of the Gibbs energy for this liquid phase will be:

$$\Delta G_{\text{liq}} = X_{1,\text{Al}}^L (\mu_{1,\text{Al}}^L - \mu_{0,\text{Al}}^L) + X_{1,\text{Si}}^L (\mu_{1,\text{Si}}^L - \mu_{0,\text{Si}}^L), \quad (5)$$

where index 1 refers to the new local composition of the liquid and index 0 – to initial composition before nucleation [9]. The total driving force will be

$$\Delta G_1(r) = \Delta G_{\text{vol}}(r) + \Delta G_{\text{surf}}(r) + \Delta G_{\text{liq}}(r). \quad (6)$$

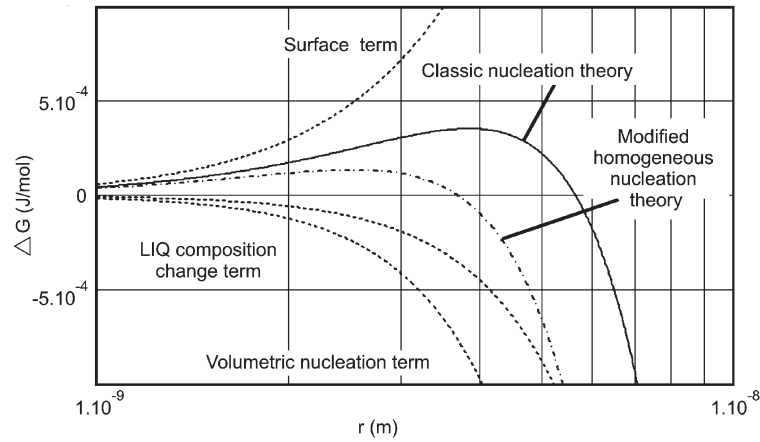


Fig. 5. Free energy contributions ( $\text{J mol}^{-1}$ ) for homogeneous nucleation of  $\beta$ -phase from the initial melt vs. nuclei radius (m) for small size range.

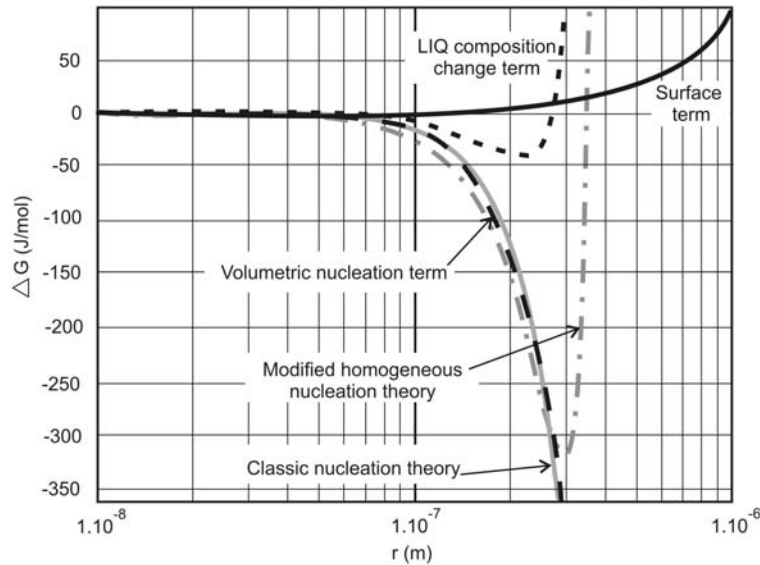


Fig. 6. Free energy contributions ( $\text{J mol}^{-1}$ ) for homogeneous nucleation of  $\beta$ -phase from the initial melt vs. nuclei radius (m) for the whole size range.

The results of calculation of these energy terms are shown in Fig. 5. It is seen that “classical” nucleation (two first terms in (6)) follows known dependence at  $r > r^*$  (critical radius  $\sim 5.6$  nm for classical Gibbs-Thomson theory and  $\sim 3.7$  nm for modified theory [9]) but deviates strongly at  $r > (15, \dots, 20)r^*$  when depletion of the liquid becomes significant (Fig. 6). It is interesting to see that the nuclei formation would theoretically be possible even if liquid composition depletes too far ( $\Delta G_{\text{liq}} > 0$ ) until total energy change ( $\Delta G_1$ ) remains negative (Fig. 6). Numerically, the difference could be seen in maximal possible nucleus radius (the second crucial radius  $r^{**}$ , which is not limited in classical theory): 283 nm to reach “equilibrium” liquidus composition and 357 nm to reach total free energy change (6) zero. Formation of nuclei of even larger size would be thermodynamically impossible due

to further positive Gibbs energy changes and too big decrease of liquid phase fraction (“dry-out”). Therefore, at these conditions above one may expect nucleation of  $\beta$ -Si in the range of radii between  $r^*$  and  $r^{**}$ .

The nucleation of  $\alpha$ -phase could be enhanced by presence of  $\beta$ -nuclei (heterogeneous nucleation [17]). Following the same logic as above, the amount of nucleated  $\alpha$ -phase could be represented as a layer of thickness  $\Delta r_{\text{Al}}$ , calculated from the volume of the precipitated  $\alpha$ -phase [10]. All the driving forces (6) can be calculated now again but with the reference to new (secondary) depleted liquid composition and counting for enrichment of the secondary liquid zone with silicon (coming not from primary  $\beta$ -nuclei but from the aluminium depletion of the liquid zone). The total driving force for the layer  $\Delta r_{\text{Al}}$  of  $\alpha$ -phase, formed on

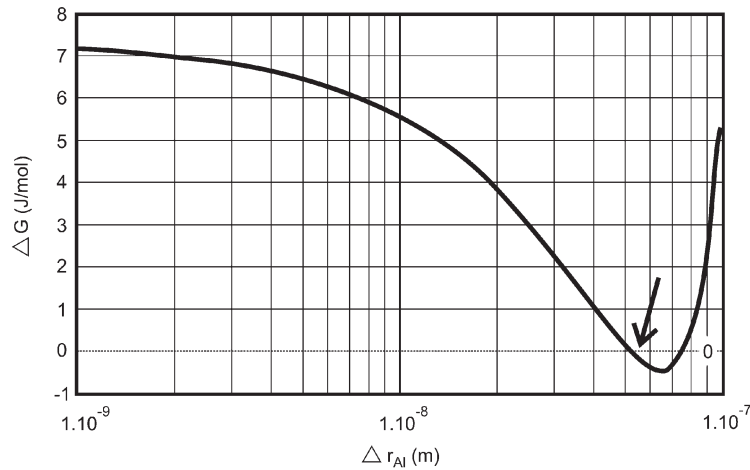


Fig. 7. Total driving force ( $\text{J mol}^{-1}$ ) of the heterogeneous nucleation of  $\alpha$ -phase layer of thickness  $\Delta r_{\text{Al}}$  (m) on the top of  $\beta$ -nucleus (for  $R_{\beta} = 356$  nm). Negative values (shown by the arrow) indicate possible nucleation limits.

the top of the nuclei of  $\beta$ -phase (assuming the latter to be constant) is shown in Fig. 7. Here it could be seen that formation of  $\alpha$ -layer of thickness till  $\Delta r_{\text{Al}}^{**} = 50\text{--}80$  nm (for these specific conditions) would be thermodynamically possible.

The stability of the formed structure (primary  $\beta$ -nuclei + shell of  $\alpha$ -phase + remaining liquid of tertiary composition) will depend on kinetics of the processes in the system and external conditions [17, 18]. Kinetics of formation of the structure observed in-situ could be stabilized if the formation of the clusters like  $\text{Al}_3\text{Si}$  [2, 3] or metastable phases like (Al, Si), JCPDS card 24-0035, in the liquid phase is taken into account. It is difficult to make evaluation of this process due to lack of thermodynamic functions of the clusters in the liquid, but a simple mass balance suggests that any process involving Si nucleation would result in clusters breakdown and immediate release of free aluminium. The latter would have a possibility to form a “freezing shell” on the nucleated Si crystal according to the simple thermodynamic reasons shown above. Undercooling, typical for chill casting and quenching, would also promote formation of such features if time for equilibration and back diffusion will be too short. The whole process would definitely affect the final microstructure and properties of the cast Al-Si alloys [16].

#### 4. Conclusions

1. *In situ* XRD analysis has been carried out for Al-21.5wt.%Si alloy during isothermal soaking at  $610^\circ\text{C}$  and primary silicon, crystalline  $\alpha$ -Al solid solution and liquid phases have been identified. The  $\alpha$ -Al solid solution has the FCC lattice with parameter  $423.8 \pm 5$  pm at  $610^\circ\text{C}$  and it was stably present in the melt over a long time soaking.

2. Microstructures of quenched from  $610^\circ\text{C}$  and as-

-cast alloy have substantial differences. There is a formation of the Al-rich shell around the silicon crystals in quenched sample.

3. The stable existence of  $\alpha$ -Al phase in semi-solid state was explained as a kinetic effect due to nucleation of silicon phase and it was shown to be thermodynamically favourable within certain limits of the nuclei size due to local depletion of the liquid phase when nucleation rate exceeds mass transport rate. Depending on the conditions, formed shell of  $\alpha$ -Al near the silicon crystals may have lower rate of dissolution and thus retains in the alloy for a long time. This would play an important role for solidification of Al-Si alloys at casting.

#### Acknowledgements

Financial support from the EU project NADIA – New automotive components designed for and manufactured by intelligent processing of light alloys (contract No. 026563-2) is gratefully acknowledged.

#### References

- [1] MAZUR, V. I.—PRIGUNOVA, A. G.—TARAN, JU. N.: Phys. Metals. Mater. Sci., 50, 1980, p. 123.
- [2] PRIGUNOVA, A. G.—MAZUR, V. I.—TARAN, JU. N.—ROSTOVSKAJA, L. A.—ROMANOVA, A. V.: Metallofizika, 5, 1983, p. 88.
- [3] PRIGUNOVA, A. G.—MAZUR, V. I.—TARAN, JU. N.—ROSTOVSKAJA, L. A.—ROMANOVA, A. V.: Metallofizika, 5, 1983, p. 54.
- [4] BUNIN, K. P.: Introduction in Metallography (in Russian). Moscow, Metallurgizdat 1954.
- [5] WANG, W.—BIAN, X.—QIN, J.—SLYUSARENKO, S.: Metal. Mater. Trans., 31A, 2000, p. 2163.
- [6] KLIUGA, A. M.—FERRANTE, M.: Acta Mater., 53, 2005, p. 345.

- [7] WARD, P. J.—ATKINSON, H. V.—ANDERSON, P. R. G.—ELIAS, L. G.—GARCIA, B.—KAHLEN, L.—RODRIGUEZ-IBABE, J.-M.: *Acta Mater.*, 44, 1996, p. 1717.
- [8] GREMAUD, M.—ALLEN, D. R.—RAPPAZ, M.—PEREPEZKO, J. H.: *Acta Mater.*, 44, 1996, p. 2669.
- [9] WASAI, K.—MUKAI, K.: *ISIJ Intern.*, 42, 2002, p. 467.
- [10] QIAN, M.: *Acta Mater.*, 55, 2007, p. 943.
- [11] TARAN, JU. N.—MAZUR, V. I.: *Structure of Eutectic Alloys*. Moscow, Metallurgy 1978.
- [12] HILLERT, M.—RETTENMEYR, M.: *Acta Mater.*, 51, 2003, p. 2803.
- [13] GILGIEN, P.—ZRYD, A.—KURZ, W.: *ISIJ Intern.*, 35, 1995, p. 566.
- [14] STIFFLER, S. R.—THOMPSON, M. O.—PEERCY, P. S.: *Phys. Rev. Lett.*, 60, 1988, p. 2519.
- [15] NEBOL'SHIN, V. A.—SHCHETININ, A. A.: *Inorg. Mater.*, 39, 2003, p. 899.
- [16] MAZUR, A. V.—GASIK, M. M.: *Kovove Mater.*, 43, 2005, p. 389.
- [17] VEHKAMÄKI, H.: *Classical Nucleation Theory in Multicomponent Systems*. Berlin-Heidelberg, Springer 2005.
- [18] KAPLAN, W. D.—KAUFMANN, Y.: *Ann. Rev. Mater. Res.*, 36, 2006, p. 1.